ACS APPLIED MATERIALS & INTERFACES

Research Article

www.acsami.org

Peptide-Capped Gold Nanoparticle for Colorimetric Immunoassay of Conjugated Abscisic Acid

Guohua Zhou, Yizhen Liu, Ming Luo, Qinfeng Xu,† Xinghu Ji, and Zhike He*

Key Laboratory of Analytical Chemistry for Biology and Medicine (Ministry of Education), College of Chemistry and Molecular Sciences, Wuhan University, Wuhan 430072, China

Supporting Information

ABSTRACT: The pentapeptide Cys-Ala-Leu-Asn-Asn (CALNN) has been proved to be a powerful tool to stabilize the AuNPs. These CALNN-capped AuNPs have been used to develop various bioanalysis platforms. In this paper, the CALNN-capped AuNPs are proved to be a robust tool for aggregation-based colorimetric immunoassays as well. A colorimetric immunoassay strategy based upon the antibody-induced assembly of functionalized AuNPs for Abscisic Acid glucose ester (ABA-GE) determination has been developed. The ABA-functionalized AuNPs aggregate in the presence of specific antibody, accompanied by a color change of the solution. The color change is competitively inhibited by ABA-GE. The interparticle distance in aggregates is small due to the thin peptide layer on the AuNPs surface, and it is determined by the "Y" shape antibody linker as well. As a result of that, an obvious color change in the immunoassays is observed. Under the optimized conditions, a linear response range from 5 nM to 10 μM for ABA-GE determination is obtained, and the limit of detection (LOD) is evaluated to be 2.2 nM. This method is simple, homogeneous, and has potential for visual detection of ABA-GE.

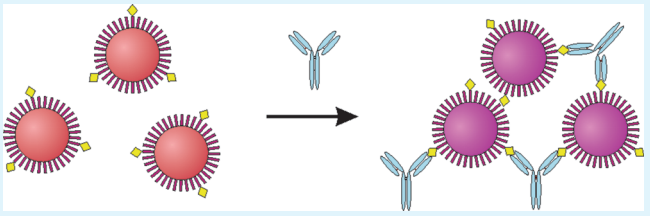

KEYWORDS: *peptide, CALNN, gold nanoparticle, colorimetric immunoassay, plant hormone, conjugated abscisic acid*

INTRODUCTION

Gold nanoparticle (AuNP)-based colorimetric assays have attracted widespread fast-growing interest in recent years because of their exquisite capability of visual detection using the naked eye.[1] The use of AuNP as a colorimetric analytical platform for various applications is based on the unique distance-dependent optical property of the AuNPs. Nanoparticle aggregates with interparticle distances substantially greater than the average particle diameter appear red, but as the interparticle distances in these aggregates decrease to less than approximately the average particle diameter, the color becomes blue.[2] Typical biosensors for different targets including DNA,[2−4] metal ions,[5,6] small molecules,[7,8] proteins,[9,10] and even cancer cells,[11,12] as well as drug screening for DNA binders[13,14] and enzyme assays[15,16] have been developed. DNA as stabilizing ligands as well as functional ligands has been widely involved in these bioanalysis. Meanwhile, the other functional molecules which have the capability to interact specifically with analytes are also employed to modify the AuNPs and establish AuNP-based colorimetric assays.[17−20] In addition, more applications of AuNP for diagnostics and detection have been well-reviewed.[21,22] It is well-known that antibodies are the most ubiquitous functional proteins that can specifically recognize antigens. The introduction of antibody to AuNP-based colorimetric assays has greatly expanded our capability to design new bioanalytical platform for almost all haptens and antigens.[23−27] However, the strategy designed for AuNP-based colorimetric immunoassays is so limited. The most popular strategy is based on that the multivalent target links the antibody-modified AuNPs by forming sandwich immunocomplex.[24−26] This approach has been extended to monovalent molecules by conjugating them to carrier molecules such as bovine serum albumin (BSA), and then linking the antibody-modified AuNPs.[23] In this case, the monovalent molecules will competitively bind to antibody-modified AuNPs, resulting in reversed color change of the solution, and thus realizing the competitive immune-detection of monovalent molecules. There is an inherent shortcoming of such strategy. The large size antibody immobilized on the surface of AuNPs enlarges the interparticle distance in aggregates. As a result of that, the interparticle distance in aggregates is larger than 25 nm and only a small color change can be observed even when large particles are used.[21] Besides, another strategy specially for competitive immunoassay of monovalent molecules is that antibody and monovalent molecule conjugated to protein are attached to nanoparticles, respectively, and then these particles aggregate without linker when they are mixed together.[27] Subsequently, the monovalent target inhibits the aggregation of nanoparticles corresponding to the concentration of target, by competitively binding to antibody. This strategy just removes one antibody from the interparticle distance. The large protein layer on the surface of AuNPs, which determines the interparticle distance has not been changed.

Received: July 19, 2012
Accepted: August 21, 2012
Published: August 21, 2012

A pentapeptide ligand, Cys-Ala-Leu-Asn-Asn (CALNN), has been proved to be a powerful tool to stabilize the AuNPs in aqueous.[28] The AuNPs with a thin CALNN self-assembled layer on the surface are extremely stable enough to be freeze-dried and stored as powders that can be subsequently redissolved to yield stable aqueous dispersions. In addition, the introduction of specific recognition group to the AuNPs can be conveniently achieved by incorporating a proportion of an appropriately functionalized peptide in addition to CALNN in the preparation process. This approach has been employed to design various bioanalysis platforms.[29−31] Regarding these, we consider that CALNN-capped AuNPs are robust tools for AuNP-based colorimetric immunoassays as well. The thin CALNN stabilizing layer will reduce the interparticle distance in aggregates greatly. Thereby, in this paper, we design a homogeneous colorimetric immunoassay for abscisic acid glucose ester (ABA-GE) using peptide-capped AuNPs.

ABA is one of the traditional plant hormones. It plays a key role in regulating plant responses to abiotic stress and in controlling seed germination, growth, and stomatal aperture.[32] ABA glucose ester (ABA-GE) is the most widespread formation of conjugated ABA.[33] It exhibits little or no biological activity in plant cells. However, in recent years, it is reported to be a transport form of ABA.[34] Thus, ABA-GE determination will help to define the relationship between ABA metabolism, plant development and environmental conditions. Recently, gas chromatography−mass spectrometer (GC-MS) and liquid chromatography−mass spectrometer (LC-MS) coupling techniques have been reported for ABA-GE determination.[35,36] Modern immunochemical methods are also mighty tools for plant hormone investigation.[37−39] These methods are sufficient in most cases as far as the sensitivity is concerned. However, GC-MS and LC-MS techniques are expensive instrument dependent, the enzyme-linked immunosorbent assays (ELISAs) require complicated protocol, and the radioimmunoassays (RIAs) have the problem of potential health hazard of radiation through the use of radioactive isotope. Therefore, an AuNP-based colorimetric immunoassay platform for simple and one-step homogeneous determination of ABA-GE will be preferred.

The strategy we reported here is based on the antibody-induced assembly of the functionalized AuNPs. In this analytical scheme, the AuNPs were functionalized with the conjugate of octapeptide and ABA, coupled by amidation reaction between the lysine residue and carboxyl group of ABA ($CALNNGK_{(ABA)}G$), as a functional ligand. These ABA−AuNPs will be linked by antibody containing two target binding sites to form aggregates. With the formation of aggregates, a red-to-purple color change can be observed. In the presence of ABA-GE, the formation of aggregate is inhibited corresponding to the concentration of ABA-GE, resulting in an inverse color change. This offers a convenient platform for ABA-GE determination. Compared with the existing analytical methods for ABA-GE determination, this developed method offers technical and operational convenience. Further details are discussed within the text.

EXPERIMENTAL SECTION

Reagents and Materials. The rabbit polyclonal antibody against ABA-GE used in experiment was obtained from the Phytohormones Research Institute, China Agricultural University, China. (+)-Abscisic acid (ABA, ∼98%) was purchased from Shanghai Kayon Biological Technology Co. Ltd., China. The peptides, Cys-Ala-Leu-Asn-Asn (CALNN, 95%) and conjugate of Cys-Ala-Leu-Asn-Asn-Gly-Lys-Gly and ABA ($CALNNGK_{(ABA)}G$, 92%), were purchased from ChinaPeptides Co. Ltd., Shanghai, China. The other reagents were all analytically pure and used without further purification. All pure water with a resistivity of 18.2 MΩ cm was purified by Milli-Q Academic purification set from Millipore.

Preparation of AuNPs. Seed AuNPs of ∼13 nm were synthesized using citrate to reduce Au^{3+} following the procedure of Grabar et al..[40] Then these particles were used as seed particles for preparation of 30.3 nm AuNPs following a procedure developed by Haiss et al.[41] In this method, Au^{3+} is reduced on the surface of preformed seed particles at room temperature using hydroxylamine−hydrochloride ($NH_2OH{\cdot}HCl$) as a reducing agent

$$HAuCl_4 + NH_2OH{\cdot}HCl \rightarrow Au + 5HCl + NO$$

The reduction of Au^{3+} on the surface of the seed AuNPs increases their diameter. The final diameter is determined by the diameter of the seed particles and the amount of reduced Au^{3+}. The 30.3 nm AuNPs we obtained were prepared by reducing 2 mL of 1% Au^{3+}. All the resulting gold colloids were stored at 4 °C in the dark to minimize photoinduced oxidation.

Preparation of ABA-Functionalized AuNPs (ABA−AuNPs). ABA−AuNPs were prepared following the procedure developed by Lévy et al..[28] A stock solution of peptide was made by dissolving the peptide in PBS (phosphate buffer saline, 160 mM NaCl, 3 mM KCl, 8 mM Na_2HPO_4, 1 mM KH_2PO_4, pH 7.2) and was kept as aliquots at −70 °C. A ligand solution was prepared by mixing CALNN and $CALNNGK_{(ABA)}G$. And subsequently, prepared AuNPs and ligand solution were mixed in a volume ratio of 10 to 1, and then incubated overnight at room temperature to obtain the ABA−AuNPs. The resulting ABA−AuNPs were purified by repeated centrifugation and redispersion in PBT (10 mM phosphate buffer containing 0.05% (v/v) Tween-20) for six times and then dispersed in PBT. The purified ABA−AuNPs can be freezing-dried and kept at −20 °C for long-term storage or be stored at 4 °C for frequent use.

Preparation of ABA-Glucose Ester (ABA-GE). ABA-GE used in this experiment was prepared following the reported procedure[42,43] with slight modification. Briefly, an aqueous solution (2.5 mL) of Cs_2CO_3 (48.9 mg, 0.15 mmol) was added to a solution of (+)-ABA (26.4 mg, 0.1 mmol) in MeOH (2.5 mL). After stirring at room temperature for 2 h, the reaction mixture was evaporated to dryness. Subsequently, the cesium salt was redissolved in DMF (3 mL), and then α-bromo-D-glucose tetraacetate (61.7 mg, 0.15 mmol) was added. The solution was kept in reflux at 60 °C until the reaction was completed. Then the mixture was diluted with water (5 mL) and extracted with EtOAc (3 × 10 mL). The combined organic extracts were washed successively with NaOH (0.1 M, 2 × 10 mL), water (2 × 10 mL) and brine (2 × 10 mL), and then concentrated under reduced pressure. Thin layer chromatograph (TLC) showed one spot of the resulting ABA-β-D-glucose tetraacetate ester. Therefore, the ABA-β-D-glucose tetraacetate ester was used for downstream reaction without further purification. Solid obtained was redissolved in NH_4OH/MeOH (v/v = 1:1, 5 mL), and reacted for 30 min at room temperature with stirring. And then the most of the solvent was evaporated, and the oily product was redissolved in EtOAc (2.5 mL). The mixture was washed with HCl (3 × 5 mL) and evaporated to dryness. The resulting solid was fractionated by preparative thin layer chromatography (EtOAc−hexanes, v/v = 1:1.5) to give ABA-β-D-glucose ester (14.5 mg, 34%).

Preparation of Real Sample. Rice of wild type was grown in green house at 23 °C for 16 h photo period. Seedlings with 10 days old were harvested. All rice leave samples were collected, weighted, immediately frozen in liquid nitrogen, and stored at −80 °C. The extraction of hormones was followed the procedure described in literature[36] except that 100 mg f.w. sample was used in extraction. Nitrogen stream dried eluate was reconstituted in 200 μL PBST (0.01 M phosphate buffer saline, containing 40 mM NaCl and 0.05% (v/v) Tween-20, pH 6.2).

Protocol of Colorimetric Immunoassay. A simple protocol of colorimetric immunoassay was described as below. Desired analyte, such as ABA-GE and ABA, was mixed with optimized antibody and ABA−AuNPs, and then incubated at 37 °C for 40 min. Then the UV−

vis spectra of properly diluted solutions were measured to obtain the absorbance of ABA−AuNPs at 640 nm (A_{640}) and the surface plasma resonance peak (A_{spr}). The procedure of the assay for real sample was identical except that the standard sample was replaced by real sample (1−5 μL).

RESULTS AND DISCUSSION

Preparation of Functionalized AuNPs. The citrate-stabilized AuNPs in large size prepared by literature method appear to be uniform sphere with small size distribution. The surface plasmon resonance peak of AuNPs red shifts from 521 to 523 nm as the size of AuNPs grows from 13 to 30.3 nm, and then it further red shifts to 526 nm after being modified with peptides (Figure 1a). This modified AuNPs is well-mono-

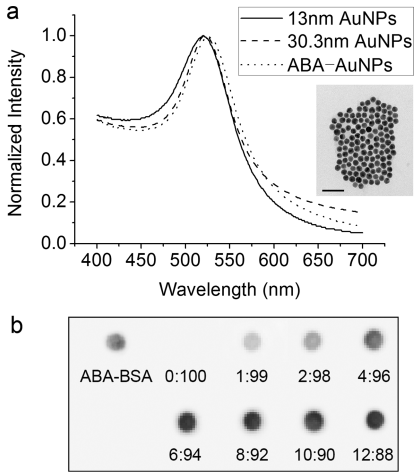

Figure 1. (a) UV−vis spectra of AuNPs and functionalized AuNPs. Inset: TEM image of the functionalized AuNPs (Bar = 100 nm). (b) Specific recognition of functionalized AuNPs with different proportion of functional ligand to CALNN by antibody.

disperse in aqueous as shown in TEM picture (Figure 1a, inset). Because the AuNPs with a self-assembled peptide monolayer on the surface resemble proteins, they are extremely stable in the aqueous state, and can be freeze-dried and stored as powders.[29] That enables the long-term storage of the functionalized AuNPs without any loss of activity. Furthermore, by varying the ratio of CALNNGK$_{(ABA)}$G to CALNN, the average number of recognition group (conjugated ABA) on the surface can be adjusted without interfering the stability of AuNPs. This allows us to investigate the influence of the number of recognition group per nanoparticle on the immunoassays.

To validate the specific recognition of ABA−AuNPs, we immobilized them on nitrocellulose membrane. The CALNN-capped AuNPs were set as negative control when the ABA-BSA conjugate was used as a positive control. This membrane was then incubated in primary antibody and peroxidase-conjugated secondary antibody, successively. The antibody raised against ABA-BSA conjugate was involved in the investigation, since it can bind conjugated ABA, and exhibits higher affinity to conjugated ABA over free ABA.[44] The chemiluminescence (CL) imaging result demonstrated the specific recognition of functionalized AuNPs by antibody and the absence of nonspecific absorption to the CALNN-capped AuNPs (Figure 1b). Additionally, the CL intensity is increased corresponding to the average number of recognition group per nanoparticle, then reaches the maturation when the CALNNGK$_{(ABA)}$G to CALNN ratio is larger then 6:94. As a result of that, the downstream experiments were conducted using the functionalized AuNPs with such ligand composition on the surface.

Agglutination of ABA−AuNPs Induced by Specific Antibody. Scheme 1 illustrates the general principle of the

Scheme 1. Scheme of AuNP-Based Colorimetric Immunoassay for ABA-GE Detection[a]

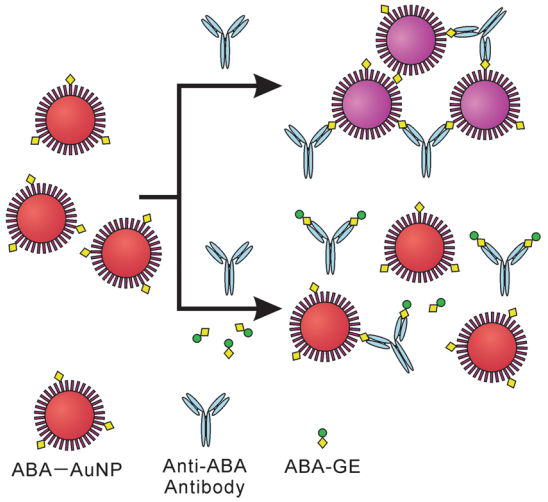

[a]Antibody induces the agglutination of ABA−AuNPs and results in a red-to-purple color change of solution. In the presence of ABA-GE, the agglutination of ABA−AuNPs is inhibited.

gold nanoparticle-based colorimetric immunoassay for ABA-GE detection. Prepared ABA−AuNPs are linked by specific antibody to form aggregates and the solutions appear to be purple. In the presence of ABA-GE, it will bind to antibody competitively and inhibit the aggregation of ABA−AuNPs, resulting in a reversed color change of the solution from purple to red. As a consequence, ABA-GE can be detected with the color variation of the solution immediately using "naked eyes" or quantified using absorption spectral measurements. First of all, the agglutination of ABA−AuNPs was investigated. As shown in Figure 2, with the increasing of antibody

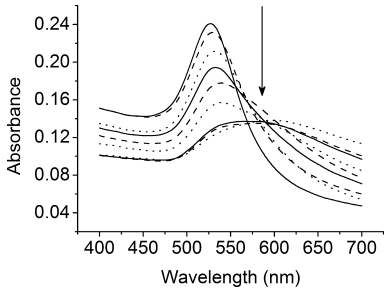

Figure 2. UV−vis spectra of ABA−AuNPs with different concentrations of antibody. The concentration of antibody was from 0.13 to 0.77 μg/mL.

concentration, the red-shifted band corresponding to the aggregated AuNPs is identified, accompanied by a decrease of absorbance at the surface plasma resonance peak and a raise at long wavelength. Therefore, a very obvious color change from red to purple is observed. This obvious color change results from a small interparticle distance in aggregates, which is attributed to the thin peptide cover of AuNPs as discussed and

the "Y" shape antibody linker. The interparticle distance between two AuNPs linked by "Y" shape antibody is determined by the angle between two Fab arms of antibody and the size of AuNPs (unpublished result). This is an advantage of the proposed method over existing AuNP-based colorimetric immunoassay strategies.

Additional evidence for the aggregation of ABA–AuNPs was accomplished via TEM imaging and DLS assays. The TEM images show that, the dispersed ABA–AuNPs assemble into expanded network with antibody. In the presence of ABA-GE, the aggregation of AuNPs was inhibited and the size of aggregates was inversely dependent on the concentration of ABA-GE (Figure 3a–e). By DLS measurements, the average

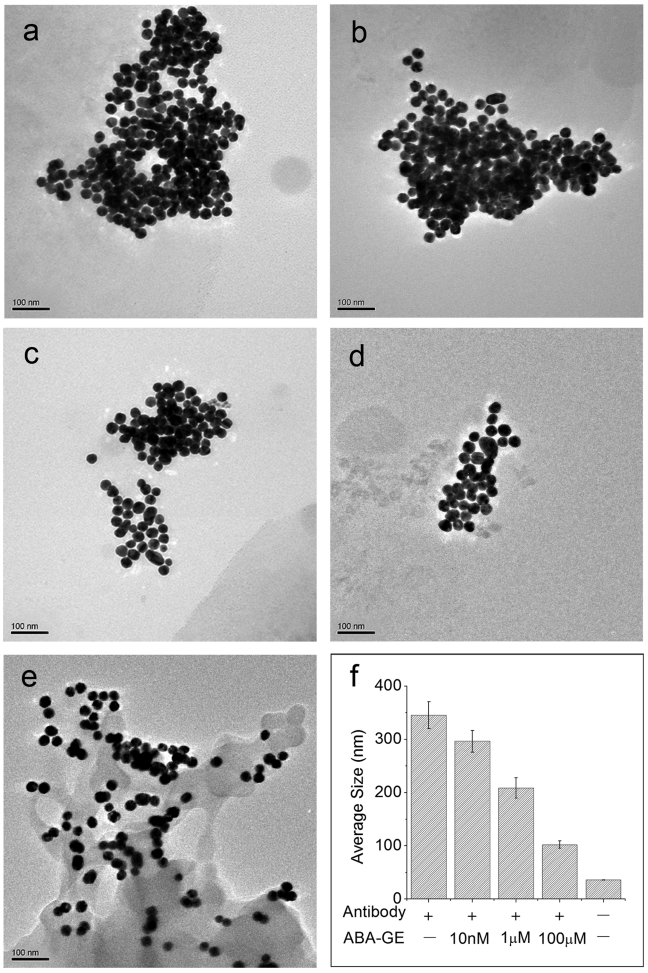

Figure 3. TEM images of (a) ABA–AuNP with antibody, ABA–AuNP with antibody in the presence of (b) 10 nM, (c) 1 μM, and (d) 100 μM ABA-GE, respectively, and (e) dispersed ABA–AuNP. (f) The corresponding average hydrodynamic diameter of particles determined by DLS measurement.

hydrodynamic diameter of ABA–AuNPs was determined to be ~36.1 nm and increased to ~345.1 nm in the presence of antibody. With the addition of ABA-GE, the average size of particle decreased gradually to ~102.2 nm corresponding to ABA-GE concentrations (Figure 3g). These results validate that the formation of ABA–AuNPs aggregates is induced by antibody, and inhibited by ABA-GE. As discussed in the text, this variation of aggregation is accompanied by a color change of the solution, and can be observed directly using "naked eyes" or by UV–vis absorbance measurements (Figure 4). With the addition of ABA-GE, the color of solution changed from purple

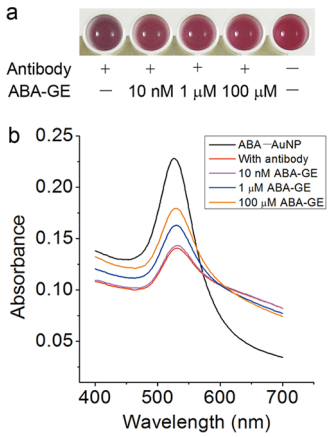

Figure 4. (a) Photograph of systems with the addition of different concentration of ABA-GE. (b) Corresponding UV–vis absorption spectra of AuNPs with different concentration of ABA-GE.

to red. Correspondingly, the UV–vis absorption spectra of AuNPs show a recovery at the surface plasma resonance peak and a decrease at long wavelength. This is the basis of the colorimetric immunoassay for ABA-GE.

Colorimetric Immunoassay of ABA-GE. The performance of presented colorimetric immunoassay for quantitative detection of ABA-GE was investigated. As literature reported, ABA-GE is extremely labile at alkaline pH.[36] However, the immunoreaction must take place at pH 6–9. To balance such a conflict, we adjusted and maintained the pH of reaction buffer solution at 6.2. Under the optimized conditions (see the Supporting Information, Figure S1), the UV–vis absorbance spectra of solutions containing deferent concentrations of ABA-GE were measured, and the ratios between A_{640} and A_{spr} were plotted to monitor the formation of aggregates. Figure 5 depicts

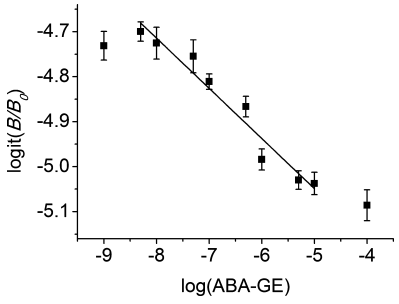

Figure 5. Calibration curve for ABA-GE determination. $B = A_{640}/A_{spr}$ of ABA–AuNP aggregate in the presence of ABA-GE, $B_0 = A_{640}/A_{spr}$ of ABA–AuNP aggregate in the absence of ABA-GE, logit (B/B_0) = LN $(B/B_0/ (100 - B/B_0))$. Error bars were standard deviation across three repetitive experiments.

the standard curve for ABA-GE quantitation. A sigmoidal curve was obtained by calculation according to literature[37] and the linear response range from 5 nM to 10 μM was illustrated. The LOD was estimated to be 2.2 nM, according to the rule of 3 times standard deviation of the blank responses (n = 7). Additionally, this method displayed favorable precision and reproducibility. The relative standard deviation (RSD) of assays

was less than 1%, and the variation between day-to-day assays was less than 10.8%.

Selectivity of Method. To further investigate the selectivity of this method, we made an attempt to compare the responses of assays to ABA and ABA-GE. ABA is the most similar and related to ABA-GE in the nature. Therefore, a comparison between ABA and ABA-GE can best manifest the selectivity of method. Mainly, these compounds at different concentrations were mixed with ABA−AuNPs and antibody, and then the A_{640}/A_{psr} of solutions was recorded after incubation under optimized conditions. As shown in Figure 6, all the curves display a concentration-dependent change of

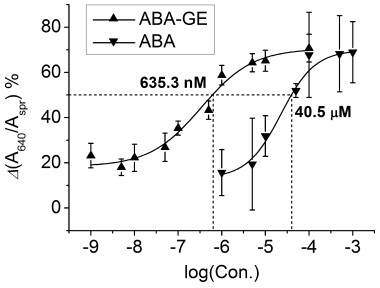

Figure 6. Correlation between A_{640}/A_{spr} and the concentration of ABA-GE and ABA, respectively. $\Delta(A_{640}/A_{spr} = (B_0 - B)/(B_0 - B_d)$. $B_d = A_{640}/A_{spr}$ of dispersed ABA−AuNP.

A_{640}/A_{psr} corresponding to the inhibition of aggregation. By measuring from the curves, the concentration of 50% inhibition can be obtained to be 635.3 nM of ABA-GE and 40.5 μM of ABA, respectively. These results are in good agreement with the literature report that the antibody shows 20−50 fold higher affinity to carboxyl-linked ABA over free ABA.[44] Therefore, we conclude that, the affinity of ABA is not high enough to interfere with the determination of ABA-GE. In other words, this method provides favorable selectivity over interference.

Application to Real Sample. To investigate the applicability of this proposed method, we had a try to evaluate the potential of this method for determining ABA-GE in a real sample. However, unexpected, some unknown components in the crude extract of rice will cause the aggregation of CALNN-capped AuNPs. As a result of that, when we performed a standard addition method in evaluation, a parallel translation of the calibration curve in real sample was observed compared with that in buffer solution (see Figure S2 in the Supporting Information). However, we believe that performing a purification of the crude extract by a correct pretreatment will certainly enable the application of this method to real samples.

Comparing with other existing analytical methods for ABA-GE detection, this proposed method has a comparable sensitivity for standard sample, as shown in Table 1. However, this method is simple, rapid, and homogeneous, and moreover, has potential for visual detection of analyte.

CONCLUSION

In summary, we used peptide-capped AuNPs to develop a simple and homogeneous colorimetric immunoassay strategy for ABA-GE determination. The AuNPs modified with CALNN as stabilizing ligand are stable, and the more important, can be functionalized conveniently. The thin peptide cover on the surface greatly reduces the interparticle distance in aggregates when the functionalized AuNPs are involved in aggregation-based colorimetric immunoassays. Besides, we employed a new strategy for determination of ABA-GE, in which the aggregation of functionalized AuNPs was induced by antibody and competitively inhibited by ABA-GE. This strategy further reduces the interparticle distance in aggregates due to the functionalized AuNPs are linked by "Y" shape antibody. Based on the investigation, a linear response range from 5 nM to 10 μM for ABA-GE determination was obtained, and the LOD was calculated to be 2.2 nM. This method shows favorable precision, reproducibility, sensitivity and selectivity. Comparing with the existing analytical methods, this proposed method is simple, rapid, homogeneous, and has potential for visual detection of ABA-GE. As a consequence, we have shown that the peptide-capped AuNPs are robust tools for developing aggregation-based colorimetric immunoassays.

ASSOCIATED CONTENT

Supporting Information

Supplementary figures and experimental detail for ABA-BSA preparation and ELISA. This material is available free of charge via the Internet at http://pubs.acs.org.

AUTHOR INFORMATION

Corresponding Author

*Tel: +86-27-68756557. Fax: +86-27-68754067. E-mail: zhkhe@whu.edu.cn.

Present Address

†Shenzhen Institutes of Advanced Technology, Chinese Academy of Sciences, Shenzhen 518055, China

Notes

The authors declare no competing financial interest.

ACKNOWLEDGMENTS

This work was supported by the National Science Foundation of China (21075093, 90717111) and the Science Fund for Creative Research Groups of NSFC (20921062). We thank Prof. Y. Feng, Mr. Y. Huang, and Miss. J. Ding for the help on rice samples.

Table 1. Comparison between this Proposed Method and Other Existing Methods for ABA-GE

	techniques	linear range (nM)	LOD for real sample(ng/g)	time consumed	reaction system	ref
1	LC−MS−MS	[a]	2.70[b]	minutes	[c]	36
2	LC−MS−MS	4.7−938.0	0.42	minutes	[c]	35
3	ELISA	1.0−100.0	1.72	hours	heterogeneous	see the Supporting Information
4	SPIA	5.0−1 × 10^4	72.07	<1 h	homogeneous	this work

[a]It is not mentioned in the reference. [b]Quantity in dry mass of sample. [c]No reaction happened during analysis procedure.

REFERENCES

(1) Zhao, W.; Brook, M. A.; Li, Y. F. *ChemBioChem* **2008**, *9*, 2363−2371.
(2) Elghanian, R.; Storhoff, J. J.; Mucic, R. C.; Letsinger, R. L.; Mirkin, C. A. *Science* **1997**, *277*, 1078−1081.
(3) Xu, W.; Xue, X. J.; Li, T. H.; Zeng, H. Q.; Liu, X. G. *Angew. Chem., Int. Ed.* **2009**, *48*, 6849−6852.
(4) Jung, C.; Chung, J. W.; Kim, U. O.; Kim, M. H.; Park, H. G. *Biosens. Bioelectron.* **2011**, *26*, 1953−1958.
(5) Xue, X. J.; Wang, F.; Liu, X. G. *J. Am. Chem. Soc.* **2008**, *130*, 3244−3245.
(6) Lee, J. S.; Han, M. S.; Mirkin, C. A. *Angew. Chem., Int. Ed.* **2007**, *46*, 4093−4096.
(7) Liu, J. W.; Lu, Y. *Angew. Chem., Int. Ed.* **2006**, *45*, 90−94.
(8) Huang, H.; Li, L.; Zhou, G.; Liu, Z.; Ma, Q.; Feng, Y.; Zeng, G.; Tinnefeld, P.; He, Z. *Talanta* **2011**, *85*, 1013−1019.
(9) Ou, L. J.; Jin, P. Y.; Chu, X.; Jiang, J. H.; Yu, R. Q. *Anal. Chem.* **2010**, *82*, 6015−6024.
(10) Pavlov, V.; Xiao, Y.; Shlyahovsky, B.; Willner, I. *J. Am. Chem. Soc.* **2004**, *126*, 11768−11769.
(11) Liu, G. D.; Mao, X.; Phillips, J. A.; Xu, H.; Tan, W. H.; Zeng, L. W. *Anal. Chem.* **2009**, *81*, 10013−10018.
(12) Kang, J.-H.; Asami, Y.; Murata, M.; Kitazaki, H.; Sadanaga, N.; Tokunaga, E.; Shiotani, S.; Okada, S.; Maehara, Y.; Niidome, T.; Hashizume, M.; Mori, T.; Katayama, Y. *Biosens. Bioelectron.* **2010**, *25*, 1869−1874.
(13) Chen, C. E.; Zhao, C. Q.; Yang, X. J.; Ren, J. S.; Qu, X. G. *Adv. Mater.* **2010**, *22*, 389−390.
(14) Hurst, S. J.; Han, M. S.; Lytton-Jean, A. K.; Mirkin, C. A. *Anal. Chem.* **2007**, *79*, 7201−7205.
(15) Xie, X.; Xu, W.; Li, T.; Liu, X. *Small* **2011**, *7*, 1393−1396.
(16) Xu, X. Y.; Han, M. S.; Mirkin, C. A. *Angew. Chem., Int. Ed.* **2007**, *46*, 3468−3470.
(17) Aili, D.; Selegard, R.; Baltzer, L.; Enander, K.; Liedberg, B. *Small* **2009**, *5*, 2445−2452.
(18) Slocik, J. M.; Zabinski, J. S., Jr.; Phillips, D. M.; Naik, R. R. *Small* **2008**, *4*, 548−551.
(19) Otsuka, H.; Akiyama, Y.; Nagasaki, Y.; Kataoka, K. *J. Am. Chem. Soc.* **2001**, *123*, 8226−8230.
(20) Radhakumary, C.; Sreenivasan, K. *Anal. Chem.* **2011**, *83*, 2829−2833.
(21) Wilson, R. *Chem. Soc. Rev.* **2008**, *37*, 2028−2045.
(22) Saha, K.; Agasti, S. S.; Kim, C.; Li, X.; Rotello, V. M. *Chem. Rev.* **2012**, *112*, 2739−2779.
(23) Leuvering, J. H. W.; Thal, P. J. H. M.; White, D. D.; Schuurs, A. H. W. M. *J. Immunol. Methods* **1983**, *62*, 163−174.
(24) Leuvering, J. H. W.; Thal, P. J. H. M.; Van der Waart, M.; Schuurs, A. H. W. M. *J. Immunol. Methods* **1981**, *45*, 183−194.
(25) Liu, X.; Dai, Q.; Austin, L.; Coutts, J.; Knowles, G.; Zou, J.; Chen, H.; Huo, Q. *J. Am. Chem. Soc.* **2008**, *130*, 2780−2782.
(26) Hirsch, L. R.; Jackson, J. B.; Lee, A.; Halas, N. J.; West, J. L. *Anal. Chem.* **2003**, *75*, 2377−2381.
(27) Zhu, Y.; Qu, C.; Kuang, H.; Xu, L.; Liu, L.; Hua, Y.; Wang, L.; Xu, C. *Biosens. Bioelectron.* **2011**, *26*, 4387−4392.
(28) Lévy, R.; Thanh, N. T. K.; Doty, R. C.; Hussain, I.; Nichols, R. J.; Schiffrin, D. J.; Brust, M.; Fernig, D. G. *J. Am. Chem. Soc.* **2004**, *126*, 10076−10084.
(29) Lévy, R. *ChemBioChem* **2006**, *7*, 1141−1145.
(30) Zhang, M.; Liu, Y.-Q.; Ye, B.-C. *Analyst* **2012**, *137*, 601−607.
(31) Gao, J.; Liu, D.; Wang, Z. *Anal. Chem.* **2010**, *82*, 9240−9247.
(32) Verslues, P. E.; Zhu, J. K. *Curr. Opin. Plant Biol.* **2007**, *10*, 447−452.
(33) Cutler, A. J.; Krochko, J. E. *Trends Plant Sci.* **1999**, *4*, 472−478.
(34) Sauter, A.; Dietz, K. J.; Hartung, W. *Plant, Cell Environ.* **2002**, *25*, 223−228.
(35) Lopez-Carbonell, M.; Gabasa, M.; Jauregui, O. *Plant Physiol. Biochem.* **2009**, *47*, 256−261.
(36) Zhou, R.; Squires, T. M.; Ambrose, S. J.; Abrams, S. R.; Ross, A. R. S.; Cutler, A. J. *J. Chromatogr. A* **2003**, *1010*, 75−85.
(37) Weiler, E. W. *Planta* **1980**, *148*, 262−272.
(38) Blintsov, A. N.; Gusakovskaya, M. A. *Russ. J. Plant Physiol.* **2006**, *53*, 407−412.
(39) Li, Q.; Wang, R. Z.; Huang, Z. G.; Li, H. S.; Xiao, L. T. *Chin. Chem. Lett.* **2010**, *21*, 472−475.
(40) Grabar, K. C.; Freeman, R. G.; Hommer, M. B.; Natan, M. J. *Anal. Chem.* **1995**, *67*, 735−743.
(41) Haiss, W.; Thanh, N. T. K.; Aveyard, J.; Fernig, D. G. *Anal. Chem.* **2007**, *79*, 4215−4221.
(42) Southwick, S. M.; Chung, A.; Davenport, T. L.; Ryan, J. W. *Plant Physiol.* **1986**, *81*, 323−325.
(43) Zaharia, L. I.; Galka, M. M.; Ambrose, S. J.; Abrams, S. R. *J. Labelled Compd. Radiopharm.* **2005**, *48*, 435−445.
(44) Hradecka, V.; Novak, O.; Havlicek, L.; Strnad, M. *J. Chromatogr. B, Anal. Technol. Biomed. Life Sci.* **2007**, *847*, 162−173.